Probabilistic Ultimate Strength Analysis of Cracked Marine-grade Aluminum Stiffened Plate Using Non-Intrusive Chaotic Radial Basis Function

Fatemeh Asadi[1,2], Ehsan Bahmyari[2*], Carlos Guedes Soares[3]

[1] *Ocean Engineering Department, Texas A&M University, USA.*

[2, *] *Faculty of Engineering, Persian Gulf University, Bushehr, Iran.*

[3] *Centre for Marine Technology and Ocean Engineering (CENTEC), Instituto Superior Técnico, Universidade de Lisboa, Avenida Rovisco Pais, 1049-001, Lisboa, Portugal*

Abstract

While ultimate strength analysis methods exist for steel marine structures, there remains a critical gap in understanding the probabilistic behavior of cracked aluminum stiffened plates, particularly in high-speed craft where operational uncertainties compound material and damage variabilities. This gap is addressed through the development of a novel probabilistic framework for analyzing the ultimate strength of cracked aluminum stiffened plates in high-speed craft by integrating nonlinear finite element analysis (NLFEA) with Non-Intrusive Chaotic Radial Basis Function (NICRBF). The framework systematically accounts for uncertainties in crack parameters (size, location, orientation) and material properties, while incorporating operational factors such as wave-induced loads and slamming effects. Through 10000 numerical simulations, it was demonstrated that crack length significantly influences ultimate strength variability (COV ranging from 0.268 to 0.353), while crack orientation affects mean ultimate stress between 253.92-295.73 MPa. For operational conditions, probability of failure increases markedly with vessel speed, reaching 0.994 at design velocity under 8m wave heights. The NICRBF approach provides an efficient computational framework while maintaining accuracy. These findings provide quantitative guidance for structural reliability assessment and safety-oriented design of high-speed aluminum vessels, particularly in determining operational limits based on wave height and speed combinations. The developed framework offers a practical tool for marine engineers to evaluate structural integrity under uncertain damage scenarios

Keywords: Aluminum Stiffened Plate, Fracture mechanics, Non-Intrusive Chaotic Radial Basis Function, Probability Analysis, Ultimate Strength.

[*] Corresponding author. Tel.: +98 7731222150; fax: +98 7733440376.

E-mail address: Ehsan.Bahmyari@pgu.ac.ir

Nomenclature

a_p	Length of the base Plate	M_u	Ultimate bending moment capacity of the structure
b_p	The breadth of the base Plate	M_t	Total bending moment acting on the structure
a_s	Length of the Stiffener	M_w	Wave-Induced bending moment
h_s	Height of the Stiffener	M_{sw}	Still water bending moment
t_p	The thickness of the Plate	M_{sl}	Slamming-induced bending moment
t_s	The thickness of the Stiffener		
σ_Y	Yield Stress (*MPa*)		
E	Modulus of Elasticity (*GPa*)		
θ_p	The angular position of the crack on the plate		
θ_s	The angular position of the crack on the Stiffener		
$P(f)$	Failure Probability		

1. Introduction

The high-speed craft sector has seen a dramatic increase in aluminum vessel construction, driven by demands for greater operational efficiency and performance. However, this shift introduces critical challenges in structural integrity assessment, particularly concerning crack damage and its probabilistic nature in marine aluminum structures. While ultimate strength-based design methods have evolved from traditional allowable-stress techniques [1], the complex behavior of cracked aluminum structures under operational conditions remains inadequately understood. The structural integrity of ship hulls becomes particularly critical in areas experiencing hogging or sagging bending moments, where the interaction between global loads and local damage mechanisms can significantly impact overall structural performance.

The Ultimate Limit State (ULS) approach, now standard in maritime structural assessment, requires careful reconsideration when applied to aluminum vessels. The distinctive advantages of the material - reduced structural weight, increased payload capacity, higher strength-to-weight ratio, and superior corrosion resistance [2] - are counterbalanced by significant challenges in structural assessment.

Material behavior differences between aluminum alloys and steel, particularly in strain-stress relationships, combined with fabrication-induced imperfections such as initial deflections, residual stresses, and material softening in the heat-affected zone (HAZ), necessitate specialized analysis approaches [2]. Most critically, aluminum alloys exhibit a crack propagation rate 30 times greater than steel under identical stress intensity factors and fatigue loading conditions [3], creating an urgent need for specialized analysis methods that can account for this accelerated damage progression.

Current modeling approaches for cracked marine aluminum structures rely predominantly on linear elastic material modeling [4-6], which inadequately captures the complex nonlinear behavior under operational conditions. The assumption of linear elasticity, while computationally efficient, fails to account for the significant plasticity effects that occur in the vicinity of crack tips and the complex interaction between material nonlinearity and geometric imperfections. While foundational experimental work by Mofflin [7] on welding effects and Clarke et al. [8] on collapse behavior provided initial insights, the specific effects of cracking damage on the ULS of aluminum structures remain insufficiently explored [8-9]. Various researchers have examined isolated aspects: Vafai et al. [10] investigated boundary conditions and crack parameters, Estekanchi et al. [5] studied buckling behavior with through cracks, and Brighenti et al. [4, 11-12] analyzed structural responses under various loading conditions. However, these studies, while valuable, have not addressed the critical need for probabilistic assessment of crack damage in marine aluminum structures.

The inherent uncertainties in crack behavior - initiation, growth, size, and orientation - combined with variabilities in welding-induced deformations, material response, age degradation, and fatigue mechanisms [13], significantly impact structural capacity. These uncertainties manifest across multiple scales: microscopic (material heterogeneity), mesoscopic (crack propagation paths), and macroscopic (global structural response). The randomness of these parameters, coupled with the stochastic nature of operational loads in high-speed craft, creates a complex reliability assessment challenge that deterministic approaches cannot adequately address. Traditional safety factor approaches, while historically useful for steel structures, may not provide adequate safety margins for aluminum structures due to their distinct failure mechanisms and greater sensitivity to damage.

This research introduces a novel integrated framework that combines Non-Linear Finite Element Modeling (NLFEM) with Non-Intrusive Chaotic Radial Basis Function (NICRBF) to analyze the probabilistic ultimate strength of cracked marine aluminum stiffened plates. The NLFEM component captures the complex material and geometric nonlinearities essential for accurate strength prediction, while the NICRBF approach provides an efficient means of handling multiple uncertain parameters

without the computational burden of traditional methods. By considering uncertainties in crack characteristics (size, location, orientation) and operational parameters (slamming loads, wave heights, vessel speeds) this study provides a comprehensive approach to structural reliability assessment. The methodology enables quantitative evaluation of failure probabilities under various operational scenarios, offering practical guidance for both design and operational decision-making in high-speed aluminum vessels.

The goal of this research is to bridge the gap between theoretical understanding and practical application in the assessment of cracked aluminum marine structures. By developing a more robust and comprehensive analysis framework, this study aims to enhance the safety and reliability of high-speed aluminum vessels while providing engineers with practical tools for structural integrity assessment under uncertain damage scenarios.

2. Ultimate Bending Moment Analysis

The buckling stress, representing the maximum load a component can sustain before instability occurs, typically falls below yielding stress and governs the overall collapse of hull girders under vertical bending moments [14]. Assessment methodologies for ultimate bending moment capacity have evolved from simplified approaches to sophisticated numerical methods, particularly for aluminum structures.

Early investigations of aluminum hull girder response employed the Smith-type progressive collapse method. Collette [1] analyzed aluminum box girder behavior under hogging bending moment using an incremental curvature approach, while Benson et al. [15] extended this methodology to account for compartment-level effects. Their comparative study validated the extended progressive collapse methodology against both conventional Smith methods and nonlinear finite element analyses at the interframe level. Further refinements in analysis techniques emerged through Magoga and Flockhart's [16] investigation of ultimate hull girder strength in aluminum high-speed patrol craft, which incorporated both vertical and horizontal bending moments using ISFEM and ALPS/HULL approaches. Significantly, their work addressed the critical influence of welding-induced imperfections, including plate and stiffener deflections, residual stresses, and HAZ material softening.

For practical design applications, Kwon et al. [17] and Kuo et al. [18] developed empirical formulations that account for buckling failure modes under sagging and hogging moments. These studies established relationships between ultimate wave bending moment (M_u) and environmental conditions through design-oriented formulae and simplified direct method. While these approaches provide valuable insights, the present study advances the field by employing numerical simulations using a systematic methodology (Figure 1) to estimate the ultimate bending moment and subsequent bending strength for a twin-hull high-speed catamaran. This approach enables more comprehensive consideration of the complex interactions between structural components and loading conditions. For a broader perspective on ultimate strength analysis of aluminum-plated structures, Hosseinabadi et al. [2] provide an extensive review of current methodologies

3. Probabilistic Failure Analysis Framework

Marine structures are subject to complex combinations of failure modes that can compromise their structural integrity during service life. Primary failure mechanisms include yielding under excessive stress, buckling under compressive loads, fatigue due to cyclic loading, and material degradation through corrosion, wear, and erosion. The interaction between these failure modes becomes particularly critical in high-speed vessels where dynamic loads and environmental factors create demanding operational conditions.

Among various structural components, stiffened panels serve as fundamental load-bearing elements in ship structures, particularly in the bottom plating and deck structures where they experience maximum compressive and tensile stresses during hogging and sagging conditions [13]. These panels, consisting of plating reinforced by longitudinal stiffeners, effectively distribute loads while maintaining structural efficiency. Their behavior under combined loading conditions provides crucial insights into the overall structural response of the vessel.

The analysis of stiffened panels offers several key advantages for structural reliability assessment. First, they represent a critical structural subsystem where multiple failure modes intersect. Second, their response characterizes the secondary behavior of the hull structure. Third, they provide a manageable scale for detailed stress distribution analysis. Finally, their failure patterns strongly correlate with overall structural performance.

For high-speed aluminum vessels, the analysis of stiffened panels becomes particularly significant due to specific material and structural characteristics. These panels demonstrate higher susceptibility to fatigue

cracking compared to steel structures, primarily due to aluminum's inherent material properties. Additionally, they show greater sensitivity to local buckling due to aluminum's lower elastic modulus. The importance of dynamic loading effects increases substantially at higher operational speeds, creating complex interactions between crack propagation and ultimate strength. These factors combine to make stiffened panel analysis crucial for understanding overall structural reliability.

This focus on stiffened panels enables the development of a comprehensive probabilistic framework that captures both local and global aspects of structural reliability while remaining computationally manageable. The present framework provides a foundation for analyzing the complex interplay between various failure modes and their impact on structural integrity.

3.1. Fundamental Limit State Function

The reliability assessment of marine structures requires a robust probabilistic framework to account for uncertainties in both load effects and structural resistance. The fundamental limit state function for structural failure can be expressed through a probabilistic formulation that considers the ultimate load-bearing capacity (M_u) and the total applied bending moment (M_t):

$$P(f) = P(M_u - M_t \leq 0) \tag{1}$$

where P(f) represents the probability of failure. This formulation defines failure as the condition where the applied loading exceeds the structural capacity, incorporating both deterministic and stochastic components of the structural response.

In marine engineering applications, the Ultimate Limit State (ULS) of overall stiffener failure represents the critical failure mode, particularly for high-speed craft where dynamic effects become significant. The total bending moment (M_t) acting on the hull girder results from the superposition of three primary components: the wave-induced moment (M_w), which captures the cyclic loading from wave action; the still-water moment (M_{sw}), which represents the static loading condition; and the slamming-induced moment (M_{sl}), which accounts for impact loads during operation.

The distinct nature of hogging and sagging conditions necessitates separate limit state functions. For the hogging condition, where the vessel experiences upward bending at midship, the limit state function is expressed as (2):

$$P(f)_{hog.} = P(M_u - \left(x_w M_w + x_{sw} M_{sw}\right) \leq 0) \tag{2}$$

For the sagging condition, which involves downward bending at midship, the limit state function incorporates additional slamming effects (3):

$$P(f)_{sag.} = P(M_u - \left(x_w M_w + x_{sw} M_{sw} + k_d k_w M_{sl}\right) \leq 0) \quad (3)$$

Here, x_w and x_{sw} serve as modeling uncertainty factors that account for inherent variabilities in wave-induced and still-water moment predictions, respectively. The dynamic load combination factors k_d and k_w modulate the interaction between various loading components, particularly significant in high-speed operations. Following established practice [19], the slamming-induced moment is considered exclusively in the sagging condition, as this represents the most critical loading scenario for bottom structures.

This probabilistic framework enables systematic incorporation of uncertainties in both loading and resistance parameters, providing a more realistic assessment of structural reliability compared to traditional deterministic approaches. The formulation accounts for the complex interaction between different loading components while maintaining mathematical tractability for practical applications.

3.2. Slamming Moment Analysis

A critical aspect distinguishing high-speed craft analysis from conventional vessel assessment is the incorporation of speed-dependent effects. While still-water and wave-induced moments remain speed-independent, the slamming moment introduces complex dynamic behavior through its explicit dependence on vertical acceleration (n_{cg}) [20]. The American Bureau of Shipping (ABS) has developed an empirical formulation for slamming moment based on extensive experimental studies [19]:

$$M_{sl} = C_3 \Delta \left(1 + n_{cg}\right)\left(LOA - l_s\right) \quad (4)$$

Where n_{cg} is the vertical acceleration of the craft at the center of gravity and is determined through the ABS experimental formula [20] as (5).

$$n_{cg} = N_2 \left(\frac{12 h_{1/3}}{N_h B_w} + 1\right) \tau \left(50 - \beta_{cg}\right) \frac{V^2 \left(N_h B_w\right)^2}{\Delta} \quad (5)$$

This formulation synthesizes multiple operational and design parameters that influence slamming loads. The hull configuration (N_h) affects the distribution of hydrodynamic forces, while the Deadrise angle (β_{cg}) determines the impact severity during water entry. The forward speed (V) and characteristic wave height ($h_{1/3}$) govern the intensity of wave encounters, with their effects modulated by the vessel displacement (Δ), and running trim (τ). The coefficients C3 and N2, calibrated through experimental validation, ensure the formulation's applicability across different vessel configurations.

3.3. Ultimate Moment Capacity

The ultimate moment capacity, representing the maximum sustainable load before structural failure, is expressed as (6):

$$M_u = \sigma_u SM \tag{6}$$

where SM represents the section modulus of the stiffened panel. This parameter is calibrated according to detailed structural analyses conducted by Kramer et al. [20], incorporating the effects of material properties, geometric configuration, and loading conditions specific to high-speed aluminum vessels.

The analysis employs parameters representative of a modern high-speed catamaran with aluminum alloy construction, as detailed in Table 1. These parameters have been selected to balance operational realism with computational efficiency, ensuring the analysis captures essential dynamic behaviors while remaining manageable.

Table 1 Vessel characteristics of the high-speed catamaran vessel [20]

Parameter	Value
Design Speed, knots	V = 34
Section Modulus	SM = 196500 cm^3
Gross Tonnage	Δ =1885 tonns
Number of hulls	N_h =2
Breadth at waterline	B_w = 25.8 m
Overall length	LOA = 96 m
The longitudinal extent of the slamming reference area	l_s = 13.54
Deadrise angle at the longitudinal center of gravity	$\beta_{cg} = 28$
Running trim at V, degrees	$\tau = 62$
Vertical acceleration at the longitudinal center of gravity	n_{cg}
Wave characteristic height	$h_{1/3}$
ABS coefficients	C_3 = 1.25 N_2 = 0.0078

The breadth at waterline (Bw) and overall length (LOA) define the primary dimensions influencing hydrodynamic behavior. The longitudinal extent of the slamming reference area (ls) determines the effective region for impact load calculations. The deadrise angle and running trim significantly affect the vessel's seakeeping characteristics and impact load distribution. The ABS coefficients C3 and N2 have been experimentally validated for this vessel configuration, ensuring reliable prediction of slamming loads under various operational conditions.

4. Uncertainty Characterization and Probabilistic Modeling

The inherently probabilistic nature of the marine environment necessitates a comprehensive treatment of uncertainties in structural analysis. Loading uncertainties arise from three primary sources: still water bending moments, wave-induced bending moments, and dynamic bending moments. The statistical characterization of these components has been extensively studied in the literature, leading to well-established probabilistic models.

The still water bending moment, primarily influenced by buoyancy and static load distribution, follows a normal distribution according to IACS 2006 [21] and Hussein et al. [22]. Wave-induced bending moments exhibit more complex statistical behavior, reflecting the stochastic nature of ocean environments. While initial studies documented in SSC-368 [23] proposed an extreme value distribution, subsequent research by Kwon et al. [17], SSC-406 [24], and Akpan et al. [25] demonstrates that a Gumbel distribution more accurately characterizes wave-induced moments (Mw). This finding has been validated across multiple vessel types and operational conditions. Model uncertainties associated with both still water and wave-induced bending moments, including nonlinear effects, are generally represented by normal distributions, as established through comprehensive statistical analyses [17, 25, 26].

Structural reliability analysis must account for uncertainties in mechanical properties and geometric parameters. Material property variations significantly impact structural performance, particularly in aluminum vessels where properties such as Young's modulus and yield stress demonstrate greater variability compared to traditional steel construction. These variations affect both local and global structural responses. Additionally, thickness variations in plates and stiffeners, arising from manufacturing processes and corrosion effects, introduce further uncertainty into strength predictions.

Crack-related uncertainties present challenges in reliability assessment. Cracks may initiate during fabrication processes or develop during service life under fatigue loading and environmental effects. The statistical characterization of crack parameters must consider their initiation, propagation, and geometric characteristics including length, orientation, and position. Following established practice in marine applications [27], these parameters are modeled using lognormal distributions, which effectively capture the non-negative nature of physical quantities while providing realistic representation of their variability.

Table 2 presents the comprehensive statistical characterization of random variables essential for reliability assessment. The yield stress and Young's modulus follow lognormal distributions with mean values of 215 MPa and 70 GPa respectively, both with coefficients of variation of 0.25. Plate and stiffener thicknesses demonstrate lower variability, with a coefficient of variation of 0.05 around a mean value of 8 mm. Crack parameters, including length and orientation, exhibit significant variability with coefficients of variation of 0.25, reflecting the inherent uncertainty in crack development and propagation.

The bending moment values demonstrate significant asymmetry between hogging and sagging conditions, reflecting the complex interaction between vessel geometry and loading conditions. The still

water bending moment reaches 90,835 kN-m in hogging while reducing to zero in sagging, demonstrating the importance of load case differentiation. Wave-induced bending moments show similar asymmetry, with values of 158,218 kN-m and 137,065 kN-m for hogging and sagging conditions respectively. These values represent typical operational conditions for high-speed aluminum vessels while accounting for the distinct characteristics of catamaran hull configurations.

Table 2 Random variables used for reliability assessment [19-20].

Parameter		Notation	Values
Yield Stress		σ_y	Lognormal, $\sigma_y(\sigma_y)$ = 215 MPa COV (σ_y) = 0.25
Young Modulus		E	Lognormal, E(E) = 70 GPa COV(E) = 0.25
Plate and stiffener thickness		t_p, t_s	Lognormal, t (t_p, t_s) = 8 COV (t_p, t_s) = 0.05
Plate Crack length		l_p	COV (0.2 b_p) = 0.25
Plate crack angle (degree)		θ_P, θ_S	Lognormal, $\theta(\theta_P, \theta_S)$ = 90 COV (θ_P,θ_S) = 0.25
Crack center position along the length		0.5 a_p	COV (0.5 a_p) = 0.25
Crack center position along the width		0.5 b_p	COV (0.5 b_p) = 0.25
Stiffener Crack length		l_s	COV (0.2 b_s) = 0.25
Still water moment modification [14], [28]		x_{sw}	Lognormal, x_{sw} (x_{sw}) = 1 COV (x_{sw}) = 0.05
Wave-induced moment modification		x_w	Lognormal, x_w (x_w) = 1 COV (x_w) = 0.15
model uncertainty in the nonlinearity of wave-induced bending moment [17]		x_s	Lognormal, x_s(x_s) = 1.15 COV (x_s) = 0.03
Wave dynamic and still water moments combination modifier		k_d	Lognormal, k_d (k_d) = 0.7 COV (x_w) = 0.15
Wave-induced and dynamic moments combination modifier		k_w	Lognormal, k_w(k_w) = 1 COV (k_w) = 0.05
Still water bending moment	For hogging For sagging	M_{sw}	90835 KN-m 0
Wave-induced bending moment	For hogging For sagging	M_w	158218 KN-m 137065 KN-m

5. Non-Intrusive Chaotic Radial Basis Function (NICRBF) Computational Framework for Uncertain Ultimate Strength Analysis

The complex interaction between mechanical properties and crack characteristics introduces significant uncertainties in ultimate strength predictions. To effectively model these uncertainties, this study employs the Non-Intrusive Chaotic Radial Basis Function (NICRBF) approach, which offers computational efficiency while maintaining accuracy in uncertainty quantification.

Based on the Chaotic Radial Basis Function methodology developed by Bahmyari and Khedmati [29] and extended by Bahmyari et al. [30], the stochastic ultimate strength of a cracked stiffened plate can be represented as:

$$M_u = \sum_{i=1}^{n} M_{ui} \emptyset_i(\xi) \tag{7}$$

Where $\boldsymbol{\xi}$ represent a *d*-dimensional random vector $\boldsymbol{\xi} = (\xi_1, \ldots, \xi_d)$ encompassing mechanical properties and crack characteristics as detailed in Table 2, *n* denotes the number of nodes in the random space and $\phi_i(\boldsymbol{\xi})$ is the shape function corresponding to the *i*-th node. This formulation provides a robust framework for capturing the complex interactions between various uncertainty parameters.

The determination of coefficients M_{ui} is crucial for calculating ultimate strength statistics. Following the non-intrusive computational scheme developed in [30, 31], these coefficients are obtained through strategic evaluations at selected points $\boldsymbol{\xi}_\alpha$. The selection of evaluation points and determination of expansion coefficients can be accomplished through various methodologies, including collocation methods and quadrature-based approaches.

This study implements a quadrature-based non-intrusive projection, formulated by multiplying Equation (7) by ϕ_i and taking the expectation:

$$< M_u \emptyset_j > \approx \sum_{\alpha=1}^{N_Q} < \emptyset_i \emptyset_j > M_{ui}, \quad j = 1, \ldots, n \tag{8}$$

The inner products in Equation (8) are evaluated through multidimensional integration schemes. Specifically, the integration in random space is approximated using Gauss quadrature:

$$< M_u \emptyset_j > \approx \sum_{\alpha=1}^{N_Q} w_\alpha M_u(\xi_\alpha) \emptyset_j(\xi_\alpha) \tag{9}$$

$$< \emptyset_i \emptyset_j > \approx \sum_{\alpha=1}^{N_Q} w_\alpha \emptyset_i(\xi_\alpha) \emptyset_j(\xi_\alpha) \tag{10}$$

where N_Q represents the number of quadrature points and ξ_α , and w_α denote the quadrature points and their corresponding weights, respectively. This integration scheme ensures both computational efficiency and numerical accuracy.

Incorporating Equations (9) and (10) into Equation (8) yields:

$$\sum_{\alpha=1}^{N_Q} w_\alpha M_u(\xi_\alpha)\emptyset_j(\xi_\alpha) = \sum_{i=1}^{n}\sum_{\alpha=1}^{N_Q} w_\alpha \emptyset_i(\xi_\alpha)\emptyset_j(\xi_\alpha)M_{ui}, \quad j = 1, \dots, n \tag{11}$$

This system can be expressed in matrix form as:

$$\begin{bmatrix} \sum_{\alpha=1}^{N_Q} w_\alpha M_u(\xi_\alpha)\phi_1(\xi_\alpha) \\ \sum_{\alpha=1}^{N_Q} w_\alpha M_u(\xi_\alpha)\phi_2(\xi_\alpha) \\ \vdots \\ \sum_{\alpha=1}^{N_Q} w_\alpha M_u(\xi_\alpha)\phi_n(\xi_\alpha) \end{bmatrix} = \begin{bmatrix} \sum_{\alpha=1}^{N_Q} w_\alpha \phi_1(\xi_\alpha)\phi_1(\xi_\alpha) & \sum_{\alpha=1}^{N_Q} w_\alpha \phi_2(\xi_\alpha)\phi_1(\xi_\alpha) & \dots & \sum_{\alpha=1}^{N_Q} w_\alpha \phi_n(\xi_\alpha)\phi_1(\xi_\alpha) \\ \sum_{\alpha=1}^{N_Q} w_\alpha \phi_1(\xi_\alpha)\phi_2(\xi_\alpha) & \sum_{\alpha=1}^{N_Q} w_\alpha \phi_2(\xi_\alpha)\phi_2(\xi_\alpha) & \dots & \sum_{\alpha=1}^{N_Q} w_\alpha \phi_n(\xi_\alpha)\phi_2(\xi_\alpha) \\ \vdots & \vdots & \ddots & \vdots \\ \sum_{\alpha=1}^{N_Q} w_\alpha \phi_1(\xi_\alpha)\phi_n(\xi_\alpha) & \sum_{\alpha=1}^{N_Q} w_\alpha \phi_2(\xi_\alpha)\phi_n(\xi_\alpha) & \dots & \sum_{\alpha=1}^{N_Q} w_\alpha \phi_n(\xi_\alpha)\phi_n(\xi_\alpha) \end{bmatrix} \begin{bmatrix} M_{u1} \\ M_{u2} \\ \vdots \\ M_{un} \end{bmatrix} \tag{12}$$

where matrix [A] and vector {b} are constructed from the quadrature points and weights. The resulting system of equations is solved using Gauss elimination to obtain the coefficients M_{ui}, enabling the complete characterization of the stochastic ultimate strength.

6. Numerical Modeling

This study investigates the stochastic behavior of ultimate strength in stiffened plates, specifically focusing on the outer bottom structure of a high-speed catamaran constructed from marine-grade aluminum alloy. Figure 1 illustrates the integrated computational framework that combines nonlinear finite element analysis (NLFEM) with the NICRBF approach to evaluate the probabilistic ultimate strength of damaged structures. This methodology enables comprehensive assessment of structural reliability while accounting for various uncertainties in geometric, material, and loading parameters.

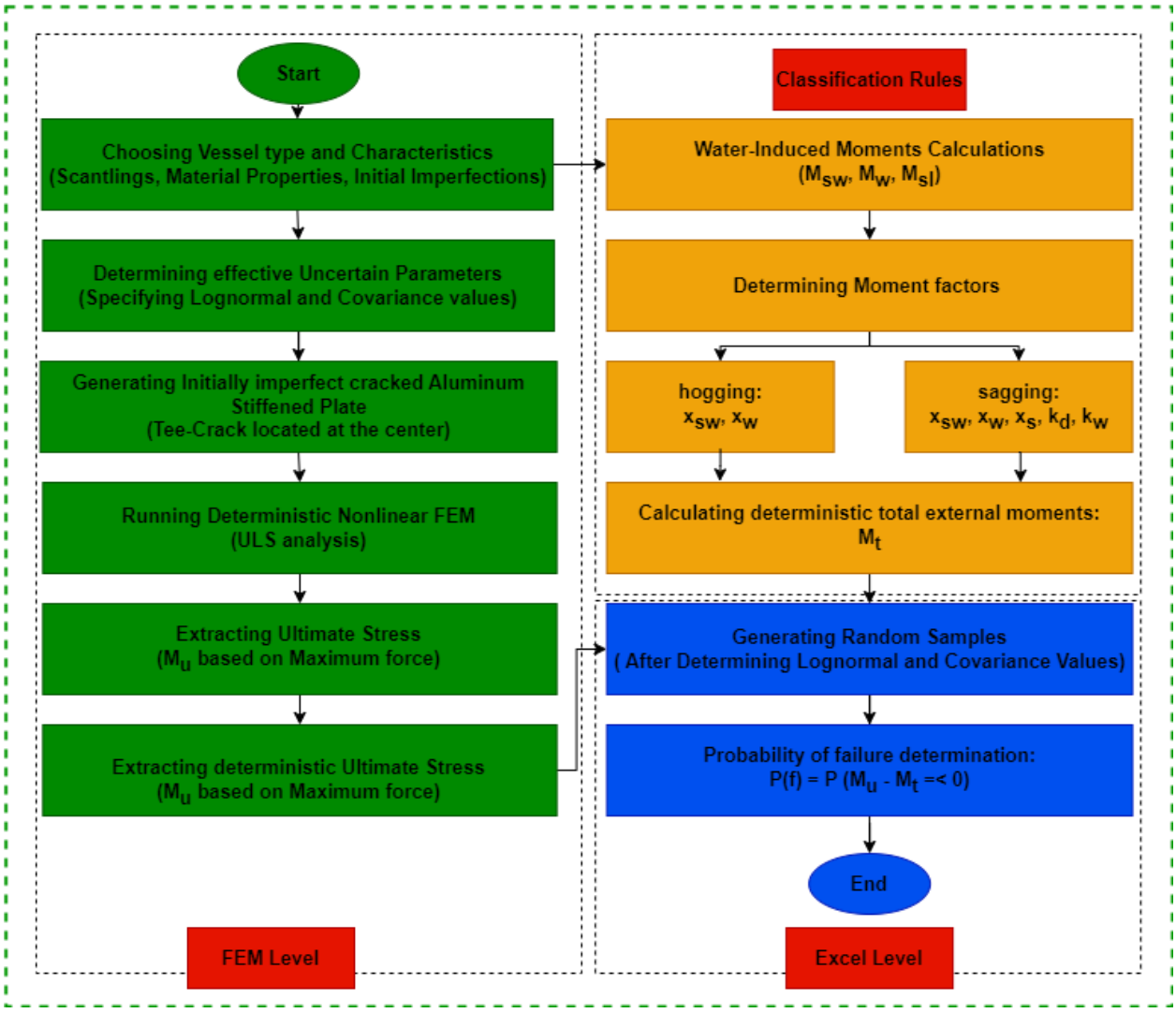

Figure 1. Computational framework integrating geometric modeling, nonlinear finite element analysis, and probabilistic methods for ultimate strength assessment of damaged aluminum ship hull structures.

The structural model comprises a stiffened plate with an initial T-crack positioned at its center. The geometric specifications of the base plate and stiffener are detailed in Table 3, while Table 4 presents the mechanical properties of the Aluminum 5083-H116 alloy employed in this study. The base plate dimensions (ap × bp × tp) and stiffener parameters (as × hs × ts) have been selected to represent typical proportions found in high-speed craft construction.

Table 3 Geometrical Dimensions

Bottom Structure		**Scantlings (*mm*)**
Base plate	(a_p× b_p × t_p)	1200 × 270 × 8
	Crack length	0.2 b_p
	Crack location	(0.5 a_p, 0.5 b_p, 0)

Flat bar stiffener	($a_s \times h_s \times t_s$)	1200 × 50 × 8
	Crack length	0.2 b_s
	Crack location	(0.5 a_s, 0, 0.5 t_s)

Table 4 Mechanical characteristics of Aluminum 5083-H116 [32]

Material	Young's Modulus [*GPa*]	Density [kg/m^3]	Poisson Ratio	Yield Stress [*MPa*]
Aluminum 5083-H116	70	2650	0.33	215

Initial imperfections, primarily introduced during welding procedures, significantly influence the structural behavior of marine aluminum structures. . Following Paik's methodology [13], initial distortions occur in three types: (1) initial deflection of plating between support members, (2) column-type, as well as (3) side-way initial deformations of the supporting elements. The magnitude and shape of each type of these distortions play important roles in buckling collapse behavior [33], and thus a better grasp of the actual imperfection configurations in the target structures is of great importance. Although methods like using experimentally measured data [34], or taking advantage of elastic buckling mode shapes [35] are commonly used as a rough estimation of the initial distortions in marine applications, Paik [13] suggests superposing the aforementioned three types of buckling mode shapes to achieve more realistic geometries. Accordingly, in this study the imperfection in the base plate is simulated as:

$$w_0^p = w_{0\,pl}\,\mathrm{Sin}\left(\frac{m\pi \mathrm{x}}{a_p}\right)\mathrm{Sin}\left(\frac{\pi \mathrm{y}}{b_p}\right) \tag{13a}$$

$$\mathrm{w}_{0\,pl} = C_1\beta^2 t_p \tag{13b}$$

$$\beta = b_p/t_p\sqrt{\sigma_Y/E} \tag{13c}$$

Where w_0^p is the initial deflection of the base plate, $w_{0\,pl}$ is its amplitude, a_p is the length of the plate along the *x-axis*, b_p is the plate span along the short edge, t_p is the plate thickness, β characterizes the slenderness ratio of the plate, E is the young's modulus of the material and σ_Y is the yield strength. Furthermore, m is the buckling half-wave number of the plate in the longitudinal direction.

Also, the stiffener experiences sideways as well as column-type initial distortions. The stiffener imperfection model incorporates both sideways and column-type initial distortions [13]:

$$w_0^S = w_{0s}\frac{z}{h_s}\mathrm{Sin}\left(\frac{\pi x}{a_s}\right) + w_{0c}\,\mathrm{Sin}\left(\frac{\pi x}{a_s}\right) \tag{14a}$$

$$w_{0s} = C_2 a_s \tag{14b}$$

$$w_{0c} = C_3 a_s \tag{14c}$$

where w_0^S is the initial deformation of the stiffener and the two terms of Eq.(14a) represent sideways and column-type initial distortion of the stiffeners, respectively. The constants in Eqs. (14b) and (14c) are defined based on the statistical evaluations of the initial deflections of welded aluminum plate. These formulations are based on statistical evaluations of welded aluminum plate deflections, ensuring realistic representation of manufacturing-induced imperfections.

The finite element analysis employs simply supported boundary conditions along transverse edges, consistent with established practices in ultimate limit state assessment. This choice is justified by previous research [24] demonstrating negligible differences between simply supported and clamped conditions under predominant longitudinal compressive loads. Figure 2 illustrates the boundary condition implementation and mesh configuration for the T-cracked stiffened plate model.

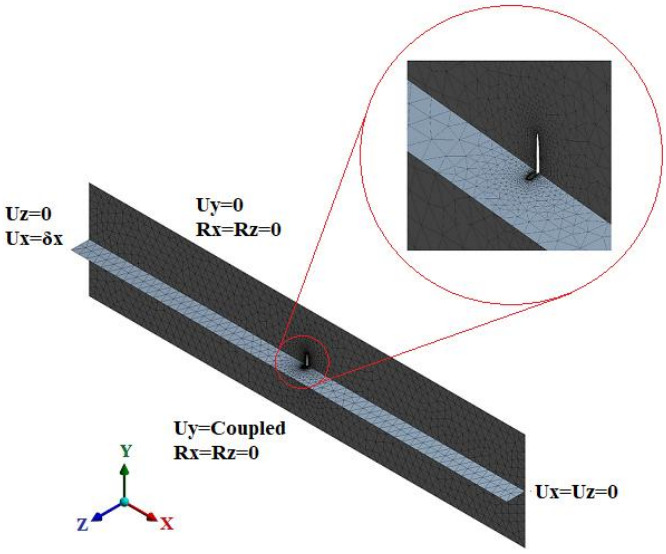

Figure 2 T-Cracked stiffened plate, boundary conditions and mesh representation

7. Results and Discussion

The probabilistic assessment of ultimate strength in marine-grade aluminum stiffened plates, conducted through non-intrusive chaotic radial basis function (NICRBF) analysis, reveals complex relationships between structural integrity and various influencing parameters. This comprehensive investigation, based on 10000 numerical simulations, examines the intricate interactions between crack characteristics, material properties, and operational conditions that determine structural reliability in high-speed vessel applications.

7.1. Effect of Crack Length on Ultimate Strength

The relationship between crack length and ultimate strength demonstrates significant nonlinearity, with important implications for structural reliability assessment. Figure 3 presents the probability density functions (PDFs) of ultimate stress for various normalized crack lengths, revealing several key findings.

At small crack lengths (0.1b), the structure exhibits relatively stable behavior with a mean ultimate stress of 309.78 MPa and coefficient of variation (COV) of 0.268. This configuration represents near-pristine conditions where crack influence remains localized. However, as crack length increases to 0.2b, two significant changes occur: the mean ultimate stress decreases to 285.32 MPa, and the COV increases substantially to 0.353. This transition marks the onset of more complex structural behavior, where crack-induced stress redistribution begins to significantly influence global structural response.

Further increases in crack length reveal unexpected patterns in structural behavior. At 0.3b, the mean ultimate stress shows a slight recovery to 290.5 MPa (COV=0.335), followed by variations at 0.4b and 0.5b with mean values of 286.09 MPa and 289.65 MPa respectively. The corresponding high COVs (0.318 and 0.351) indicate persistent variability in structural response. This non-monotonic relationship between crack length and ultimate strength suggests complex interaction mechanisms involving stress redistribution around crack tips, load transfer patterns through the stiffened plate system, local-global interaction effects in the structural response, and evolution of effective load-bearing paths as crack length increases.

The observed behavior patterns have significant implications for structural design and assessment. The increasing COV values with crack length indicate growing uncertainty in strength predictions, necessitating more conservative safety factors for longer cracks. Furthermore, the non-monotonic relationship between crack length and mean ultimate strength challenges traditional assumptions about progressive degradation of structural capacity with increasing damage.

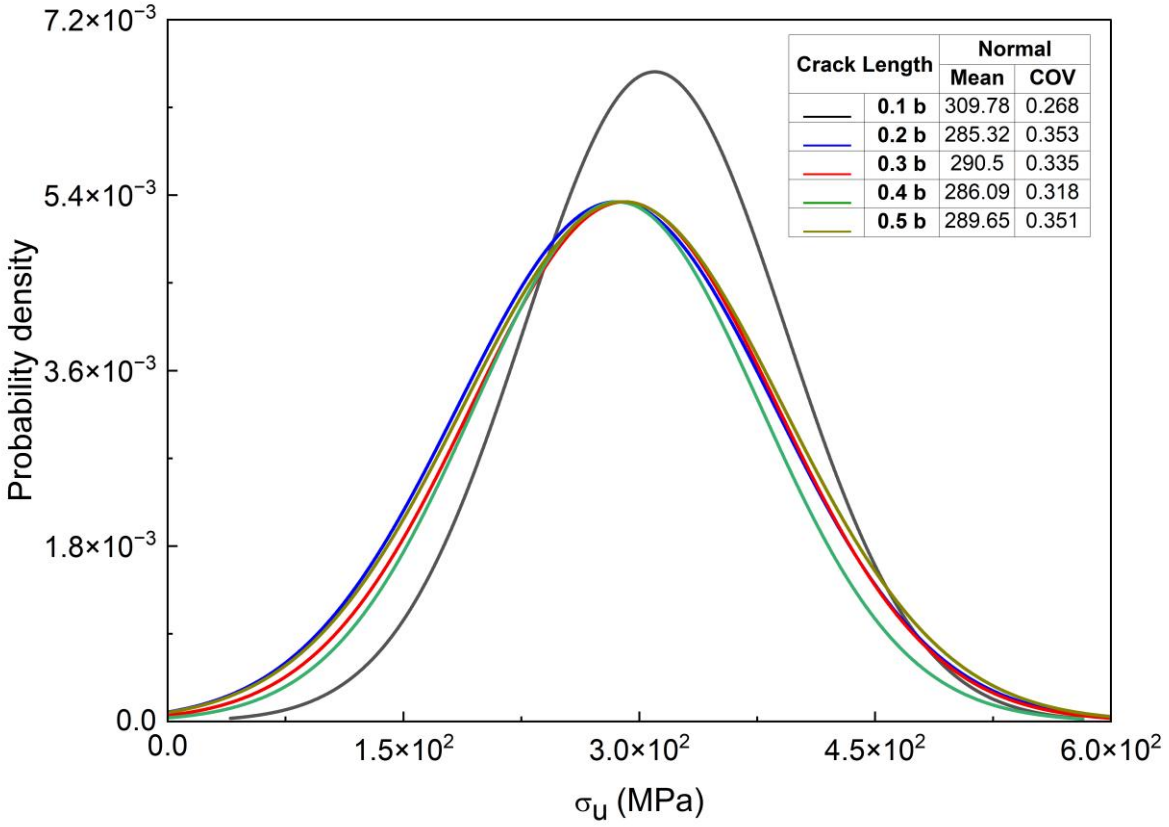

Figure 3 Probability density functions of ultimate strength for a marine-grade aluminum stiffened plate with varying crack length ratios (a/b = 0.1-0.5).

This analysis marks a significant advance in understanding the probabilistic nature of structural response in damaged marine structures. The combination of detailed PDF analysis with physical interpretation of structural behavior provides valuable insights for both design practice and theoretical understanding of damage mechanics in stiffened plate systems.

7.2. Effect of Crack Orientation on Ultimate Strength

The angular orientation of cracks significantly influences the ultimate strength characteristics of marine aluminum stiffened plates, revealing complex relationships between crack geometry and structural performance. Figure 4 presents probability density functions of ultimate strength for crack angles ranging from 15° to 90°, demonstrating distinct behavioral patterns across different orientations.

Analysis of crack angles between 15° and 45° reveals a gradual transition in structural response characteristics. At 15°, the structure exhibits a mean ultimate stress of 294.28 MPa with a COV of 0.338,

indicating moderate variability in strength distribution. A slight reduction in both mean ultimate stress (293.27 MPa) and COV (0.336) occurs at 30°, followed by a further decrease at 45° to 289.86 MPa (COV=0.311). This progressive reduction in both mean strength and variability suggests a systematic change in load transfer mechanisms as crack orientation shifts.

The structural response demonstrates notable nonlinearity at intermediate angles. At 60°, the mean ultimate stress increases unexpectedly to 295.73 MPa (COV=0.331), indicating enhanced load-bearing capacity. This phenomenon may be attributed to more favorable stress redistribution patterns at this orientation. However, a dramatic reduction occurs at 75°, where the mean ultimate stress drops to 253.92 MPa with the lowest observed COV of 0.278, suggesting a fundamental change in the structural response mechanism.

Perpendicular crack orientation (90°) produces distinct behavioral characteristics, with mean ultimate stress recovering to 285.32 MPa but exhibiting the highest variability (COV=0.353). This combination of moderate strength and maximum uncertainty indicates complex interaction between crack orientation and load-bearing mechanisms at right angles to the primary loading direction.

The observed variations in ultimate strength with crack angle demonstrate the necessity of incorporating orientation effects in structural reliability assessments. The non-monotonic relationship between crack angle and ultimate strength challenges conventional assumptions about damage criticality. Furthermore, the significant changes in COV across different orientations suggest that reliability analyses must account for orientation-dependent uncertainty in strength predictions.

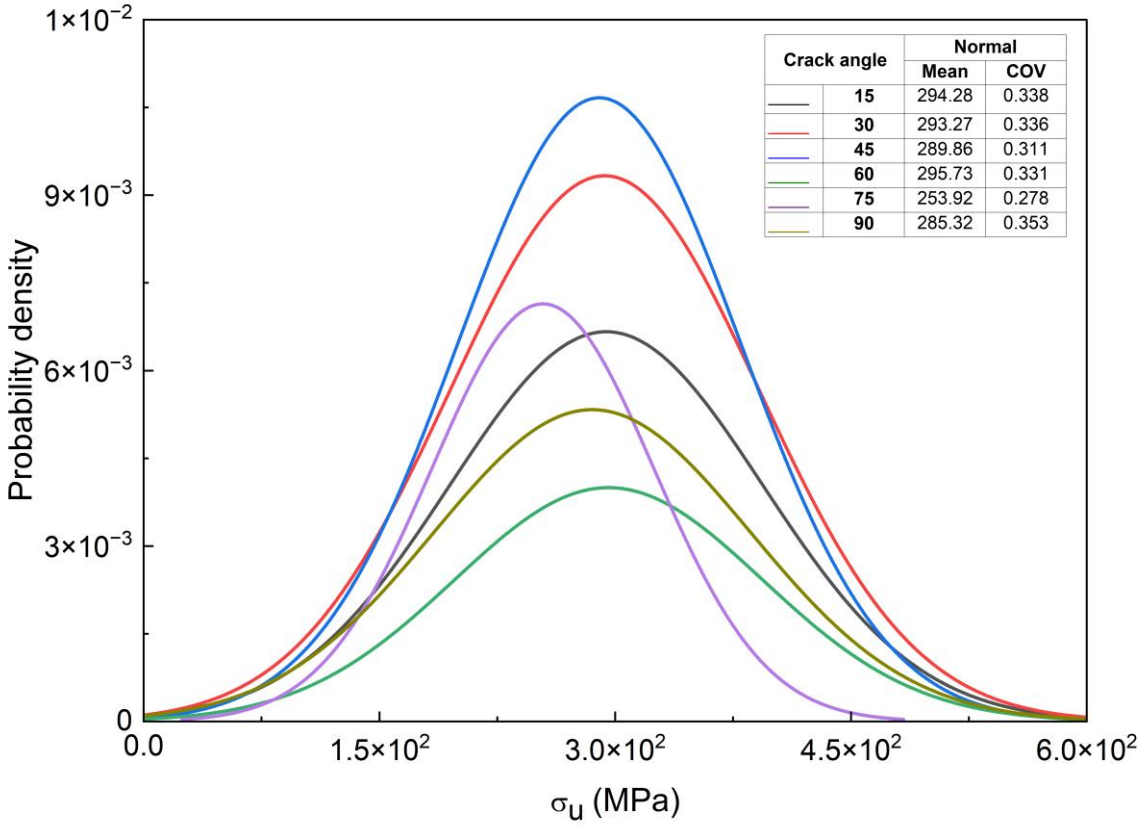

Figure 4 Probability density functions of ultimate strength for marine-grade aluminum stiffened plates with varying crack orientations (15°-90°).

These findings advance the understanding of orientation-dependent damage effects in marine structures and provide quantitative basis for implementing orientation-specific safety factors in design procedures. The demonstrated complexity of the strength-orientation relationship emphasizes the importance of comprehensive probabilistic analysis in structural assessment of damaged marine components.

7.3. Effect of Crack Position on Ultimate Strength

The spatial distribution of cracks along the stiffened plate length introduces significant variations in structural response characteristics, revealing location-dependent patterns in ultimate strength behavior. Statistical analysis of crack positions, normalized to plate length L, demonstrates systematic transitions in both strength magnitude and variability.

Near the plate edge (0.1L), the structure exhibits a mean ultimate strength of 211.24 MPa with a COV of 0.281, representing baseline behavior where edge effects and crack interaction remain partially

decoupled. As crack position shifts to 0.2L, mean ultimate strength increases to 219.17 MPa, accompanied by increased variability (COV=0.341). This transition indicates the emergence of more complex stress distribution patterns as the crack moves into regions of greater structural interaction.

The structural response demonstrates remarkable sensitivity to crack position in the intermediate region. At 0.3L, mean ultimate strength continues its upward trend to 225.94 MPa while experiencing reduced variability (COV=0.211), suggesting a region of enhanced structural stability. However, a dramatic transition occurs at 0.4L, where mean ultimate strength reaches its maximum at 291.91 MPa but exhibits the highest observed variability (COV=0.367). This combination of peak strength and maximum uncertainty reveals critical interaction between crack position and stiffening elements.

At mid-length (0.5L), the structure maintains elevated strength levels (258.32 MPa) with persistent high variability (COV=0.353). This behavior pattern indicates sustained complex interaction between crack-induced stress fields and structural stiffening elements, resulting in less predictable response characteristics. The observed strength variations correlate with changing stress concentration patterns and modified load transfer mechanisms across stiffening elements.

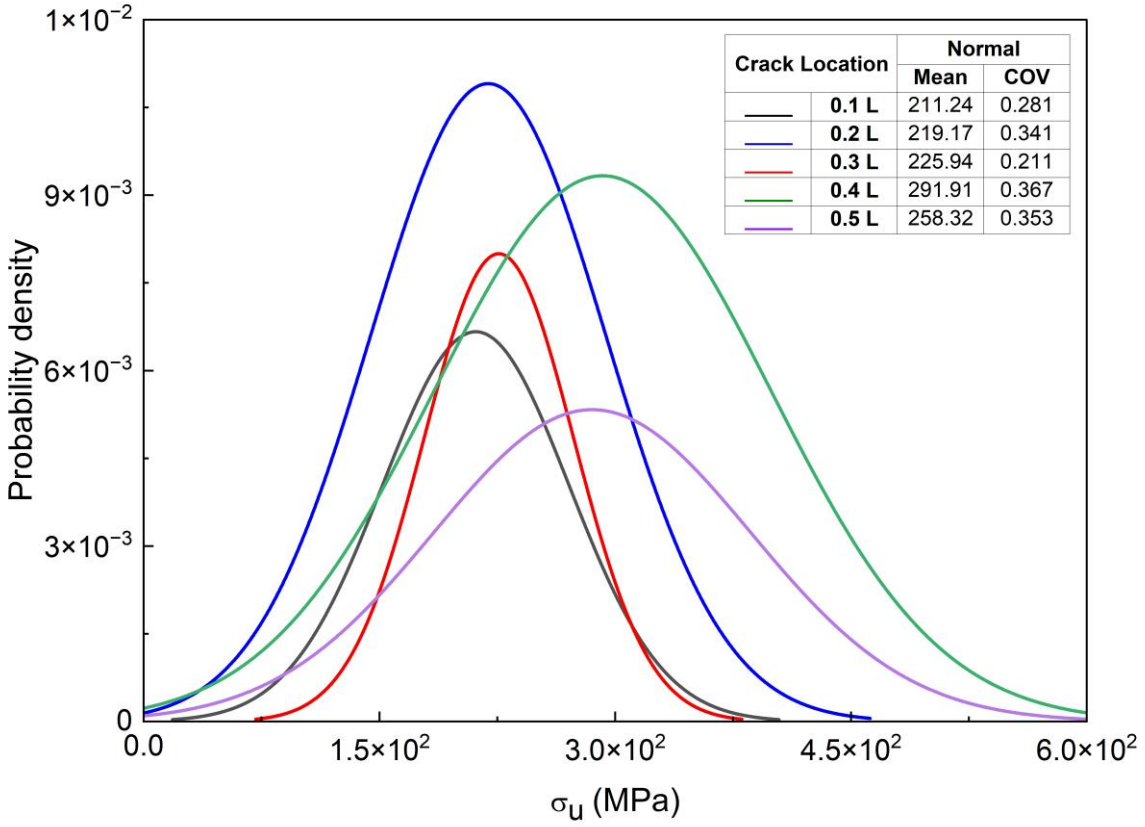

Figure 5 Probability density functions of ultimate strength for marine-grade aluminum stiffened plates with varying crack locations (0.1L-0.5L) along weld line.

These findings establish quantitative relationships between crack position and structural reliability, demonstrating the importance of location-specific analysis in damage assessment procedures. The identified patterns of strength variation with crack position provide essential insights for developing position-dependent safety factors and inspection protocols in marine structural systems.

8. Operational Analysis of High-Speed Catamaran Structure

8.1. Stochastic Analysis Framework

The structural reliability assessment employed a comprehensive stochastic approach through 10000 numerical simulations, encompassing multiple parameter variations. Material properties (Young's modulus, yield strength), geometric characteristics (crack length, angle, position in both plate and stiffener), and dimensional parameters (plate and stiffener thickness) were systematically varied to capture inherent uncertainties. The analysis incorporated operational uncertainties through still water and wave-induced

moments, examining four distinct vessel speeds (0.25Vd, 0.5Vd, 0.75Vd, and design velocity Vd) across wave heights ranging from 1 to 8 meters.

8.2. Sagging Condition Analysis

The relationship between probability of failure and operational conditions under sagging demonstrates complex nonlinear behavior, as shown in Figure 6(a). At low operational speed (0.25Vd), the structure maintains remarkable stability, with negligible failure probability across all wave heights. This robust performance stems from reduced wave-induced moments, resulting in stress states well below critical thresholds.

As vessel speed increases to 0.5Vd, a clear transition in structural reliability emerges. The probability of failure increases from 0.002 at 1-meter wave height to 0.093 at 8 meters, marking the onset of significant wave-induced stress effects. While these values indicate maintained structural integrity, they reveal growing sensitivity to environmental conditions.

Operation at 0.75Vd introduces substantially higher risk levels. The failure probability rises markedly from 0.083 at 1-meter wave height to 0.775 at 8 meters. This sharp increase reflects the compounded effects of increased velocity and wave height, with dynamic loads approaching structural capacity limits. The substantial rise in failure probability indicates a critical transition in structural behavior, where speed-induced loads begin to dominate the response characteristics.

At design velocity (Vd), structural vulnerability becomes severe across all operational conditions. Initial failure probability at 1-meter wave height reaches 0.517, escalating rapidly to 0.994 at 8 meters. This behavior pattern reveals fundamental limitations in current design methodologies for high-speed operations in severe sea states. Even moderate wave conditions produce failure probabilities exceeding typical design thresholds, necessitating careful operational restrictions.

8.3. Hollow Landing Analysis

The hollow landing condition analysis, presented in Figure 6(b), reveals distinct vulnerability patterns across operational speeds. At 0.25Vd, structural integrity remains intact across all wave heights, demonstrating effective load management at reduced speeds. The transition to 0.5Vd introduces moderate risk levels, with failure probability increasing from zero at 1 meter to 0.081 at 8-meter wave height.

Operation at 0.75Vd demonstrates markedly different behavior characteristics. Initial failure probability of 0.017 at 1-meter wave height increases dramatically to 0.835 at 8 meters. This significant escalation reflects enhanced sensitivity to wave-induced loading at higher operational speeds. The relationship between wave height and failure probability becomes increasingly nonlinear, indicating complex interaction between speed-dependent loads and structural response mechanisms.

Design speed operations under hollow landing conditions reveal critical vulnerability thresholds. Initial failure probability of 0.608 at 1-meter wave height rapidly increases to unity at 6 meters, maintaining

maximum risk through 8-meter conditions. This behavior pattern indicates a fundamental limit state where combined speed and wave effects consistently exceed structural capacity.

8.4. Implications for Design and Operation

These comprehensive findings establish quantitative relationships between operational parameters and structural reliability in high-speed marine vessels. The analysis reveals critical thresholds in both sagging and hollow landing conditions, providing essential guidance for operational limits and design criteria. The demonstrated sensitivity to combined speed and wave height effects necessitates careful consideration in both vessel operation protocols and structural design specifications.

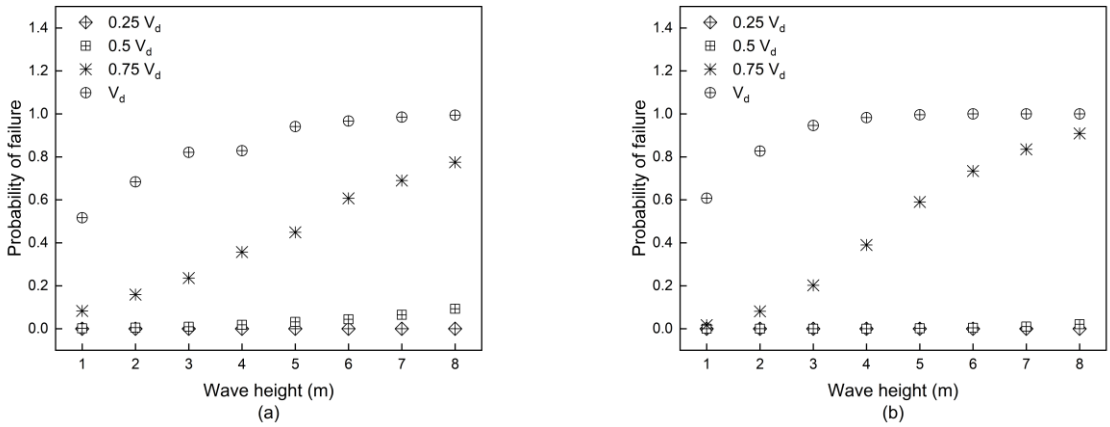

Figure 6 Probability of failure analysis for marine-grade aluminum stiffened plates under (a) sagging and (b) hollow landing conditions, showing speed-dependent response (0.25Vd-Vd) across wave heights (1-8 m).

9. Conclusion

This investigation advances the understanding of ultimate strength characteristics in marine-grade aluminum stiffened plates through integration of nonlinear finite element analysis with Non-Intrusive Chaotic Radial Basis Function (NICRBF) methodology. Several significant conclusions emerge from this research:

The developed computational framework demonstrates remarkable effectiveness in capturing the complex interactions between crack damage, operational conditions, and structural response. Through systematic analysis of 10,000 random samples, the NICRBF approach reveals previously unidentified relationships between crack characteristics and ultimate strength behavior. Crack length emerges as the dominant parameter influencing both failure probability and reliability index, confirming deterministic predictions through probabilistic validation.

Analysis of crack orientation and location effects reveals unexpected patterns in structural response. The ultimate strength demonstrates nonlinear dependence on crack angle, with critical transitions occurring at

specific orientations. These findings challenge conventional assumptions about damage criticality and necessitate more nuanced approaches to structural assessment.

The investigation of operational parameters yields crucial insights for maritime applications. Vessel speed and wave height emerge as critical factors governing structural reliability, with their combined effects producing nonlinear amplification of failure probability. In sagging conditions, failure probability increases from negligible levels at quarter-speed to near-certainty at design speed under extreme wave conditions. Hollow landing analysis reveals even more pronounced sensitivity to operational parameters, with failure probability reaching unity at moderate wave heights during high-speed operations.

The study establishes quantitative relationships between crack configurations and structural reliability across various operational conditions. These relationships provide essential guidance for:

1. Development of speed-dependent operational limits
2. Establishment of wave height restrictions for high-speed vessels
3. Implementation of damage-tolerant design approaches
4. Enhancement of inspection and maintenance protocols

This research contributes fundamental advances in three key areas: probabilistic modeling of damaged marine structures, understanding of speed-dependent failure mechanisms, and development of reliability-based design criteria. The demonstrated effectiveness of the NICRBF approach in capturing complex stochastic behavior establishes a robust framework for future developments in ultimate strength assessment methodology.

The findings emphasize the critical importance of incorporating probabilistic analysis in marine structural design, particularly for high-speed aluminum vessels operating in demanding conditions. Future research should focus on extending this methodology to more complex structural configurations and operational scenarios, further advancing the field of reliability-based marine structural design.

References

[1] M. D. Collette, “The Impact of Fusion Welds on the Ultimate Strength of Aluminum Structures,” in *10th International Symposium on Practical Design of Ships and Other Floating Structures*, 2007.

[2] O. F. Hosseinabadi and M. R. Khedmati, “A review on ultimate strength of aluminium structural elements and systems for marine applications,” *Ocean Eng.*, vol. 232, no. April, p. 109153, 2021, doi: 10.1016/j.oceaneng.2021.109153.

[3] R. Sielski, “Research needs in aluminum structure,” *Ships Offshore Struct.*, vol. 3, no. 1, pp. 57–65, 2008, doi: 10.1080/17445300701797111.

[4] R. Brighenti, “Numerical buckling analysis of compressed or tensioned cracked thin plates,” *Eng. Struct.*, vol. 27, no. 2, pp. 265–276, 2005, doi: 10.1016/j.engstruct.2004.10.006.

[5] H. E. Estekanchi and A. Vafai, “On the buckling of cylindrical shells with through cracks under axial load,” *Thin-Walled Struct.*, vol. 35, no. 4, pp. 255–274, 1999, doi: 10.1016/s0263-8231(99)00028-2.

[6] J. K. Paik, Y. V. S. Kumar, and J. M. Lee, “Ultimate strength of cracked plate elements under axial compression or tension,” *Thin-Walled Struct.*, vol. 43, no. 2, pp. 237–272, 2005, doi: 10.1016/j.tws.2004.07.010.

[7] D. S. Mofflin, “Plate buckling in steel and aluminium.,” University of Cambridge, 1983.

[8] J. Clarke and J. Swan, “Interframe buckling of aluminum alloy stiffened plating,” 1985, Accessed: Nov. 13, 2022. [Online]. Available: https://apps.dtic.mil/sti/citations/ADA163808.

[9] F. H. Clarke and G. R. Munro, “Coastal States, Distant Water Fishing Nations And Extended Jurisdiction: A Principal–Agent Analysis,” *Nat. Resour. Model.*, vol. 2, no. 1, pp. 81–107, Jun. 1987, doi: 10.1111/J.1939-7445.1987.TB00027.X.

[10] A. Vafai and H. E. Estekanchi, “Parametric finite element study of cracked plates and shells,” *Thin-Walled Struct.*, vol. 33, no. 3, pp. 211–229, 1999, doi: 10.1016/S0263-8231(98)00042-1.

[11] R. Brighenti and A. Carpinteri, “Buckling and fracture behaviour of cracked thin plates under shear loading,” *Mater. Des.*, vol. 32, no. 3, pp. 1347–1355, 2011, doi: 10.1016/j.matdes.2010.09.018.

[12] R. Brighenti, “Buckling sensitivity analysis of cracked thin plates under membrane tension or compression loading,” *Nucl. Eng. Des.*, vol. 239, no. 6, pp. 965–980, 2009, doi: 10.1016/j.nucengdes.2009.01.008.

[13] J. K. Paik, *Ultimate Limit State Analysis and Design of Plated Structures*. 2018.

[14] J. K. Paik and A. E. Mansour, “A simple formulation for predicting the ultimate strength of ships,” *J. Mar. Sci. Technol. 1995 11*, vol. 1, no. 1, pp. 52–62, Feb. 1995, doi: 10.1007/BF01240013.

[15] S. Benson, J. Downes, and R. S. Dow, “Ultimate strength characteristics of aluminium plates for high-speed vessels,” *Ships Offshore Struct.*, vol. 6, no. 1–2, pp. 67–80, 2011, doi: 10.1080/17445302.2010.529696.

[16] T. Magoga and C. Flockhart, “Effect of weld-induced imperfections on the ultimate strength of an aluminium patrol boat determined by the ISFEM rapid assessment method,” *Ships Offshore Struct.*,

vol. 9, no. 2, pp. 218–235, 2014, doi: 10.1080/17445302.2013.768524.

[17] K. Kwon and D. M. Frangopol, “System reliability of ship hull structures under corrosion and fatigue,” *Trans. - Soc. Nav. Archit. Mar. Eng.*, vol. 120, pp. 603–620, 2013.

[18] H.-C. Kuo Associate Professor and J.-R. Chang Associate Professor, “A Simplified Approach to Estimate the Ultimate Longitudinal Strength of Ship Hull,” *J. Mar. Sci. Technol.*, vol. 11, 2003, doi: 10.51400/2709-6998.2272.

[19] American Bureau of Shipping, “Slamming loads and strength assessment for vessels,” *Assessment*, vol. 2011, no. March, p. 36, 2011.

[20] R. K. Kramer, C. McKesson, J. McConnell, W. Cowardin, and B. Samuelsen, “Structural Optimization for Conversion of Aluminium Car Ferry to Support Military Vehicle Payload,” *Sh. Struct. Comm.*, 2005, [Online]. Available: internal-pdf://0173570718/438 complete.pdf.

[21] IACS, “Common Structural Rules for Double Hull Oil Tankers Rules SAFER,” no. January, 2006.

[22] A. W. Hussein and C. Guedes Soares, “Reliability and residual strength of double hull tankers designed according to the new IACS common structural rules,” *Ocean Eng.*, vol. 36, no. 17–18, pp. 1446–1459, Dec. 2009, doi: 10.1016/J.OCEANENG.2009.04.006.

[23] Ship Structural Committee, “Ssc-368 Probability-Based Ship Design (Phase I): A Demonstration,” 1993.

[24] I. F. Glen, R. B. Paterson, and L. Luznik, “SSC-406: Sea Operational Profiles For Structural Reliability Assessment,” p. 114, 1999.

[25] U. O. Akpan, T. S. Koko, B. Ayyub, and T. E. Dunbar, “Risk assessment of aging ship hull structures in the presence of corrosion and fatigue,” *Mar. Struct.*, vol. 15, no. 3, pp. 211–231, May 2002, doi: 10.1016/S0951-8339(01)00030-2.

[26] A. E. Mansour and L. Hovem, “Probability-Based Ship Structural Safety Analysis,” *J. Sh. Res.*, vol. 38, no. 4, pp. 329–339, 1994.

[27] G. Q. Feng, Y. Garbatov, and C. Guedes Soares, “Probabilistic model of the growth of correlated cracks in a stiffened panel,” *Eng. Fract. Mech.*, vol. 84, pp. 83–95, Apr. 2012, doi: 10.1016/J.ENGFRACMECH.2012.01.008.

[28] “SSC 398- Assessment of Reliability of Ship Structures,” 1997.

[29] Bahmyari, E., Khedmati, M.R. Uncertainty quantification in bending analysis of moderately thick

plates with elastically restrained edges using the Chaotic Radial Basis Function. *Acta Mech* **228**, 2083–2105 (2017). https://doi.org/10.1007/s00707-017-1822-7

[30] Ehsan Bahmyari, Free and forced vibration analysis of moderately thick plates with uncertain material properties using the Chaotic Radial Basis Function, Engineering Analysis with Boundary Elements,Volume 106, 2019, Pages 349-358

[31] Bahmyari, E. Stochastic Vibration Analysis of Laminated Composite Plates with Elastically Restrained Edges Using the Non-Intrusive Chaotic Radial Basis Function. *Iran J Sci Technol Trans Mech Eng* **47**, 285–305 (2023). https://doi.org/10.1007/s40997-022-00511-2

[32] Bahmyari, E., Soares, C.G. Uncertainty Quantification in Free Vibration Analysis of Cracked Moderately Thick Plates Using the Non-intrusive Chaotic Radial Basis Function. *J. Vib. Eng. Technol.* **11**, 599–618 (2023). https://doi.org/10.1007/s42417-022-00597-7

[33] B. C. Cerik, "Large inelastic deformation of aluminium alloy plates in high-speed vessels subjected to slamming," *J. Mar. Sci. Technol.*, vol. 22, pp. 301–312, 2017, doi: 10.1007/s00773-016-0411-0.

[34] J. Paik, A. Thayamballi, J. L.-J. of S. Research, and undefined 2004, "Effect of initial deflection shape on the ultimate strength behavior of welded steel plates under biaxial compressive loads," *onepetro.org*, Accessed: Sep. 28, 2021. [Online]. Available: https://onepetro.org/JSR/article-abstract/48/01/45/175000.

[35] M. Kmiecik, T. Jastrzębski, and J. Kuzniar, "Statistics of ship plating distortions," *Mar. Struct.*, vol. 8, no. 2, pp. 119–132, Jan. 1995, doi: 10.1016/0951-8339(94)00014-J.

[32] J. K. Paik, "Residual ultimate strength of steel plates with longitudinal cracks under axial compression-Nonlinear finite element method investigations," *Ocean Eng.*, vol. 36, no. 3–4, pp. 266–276, 2009, doi: 10.1016/j.oceaneng.2008.12.001.

Appendix A: Numerical Model Validation and Mesh Convergence Analysis

A.1 Ultimate Strength Model Validation

The numerical model's accuracy was validated against established finite element results from Paik [6] for a 1000×1000 mm shell panel under two critical configurations: an intact plate and a cracked plate with normalized crack length 2c/b = 0.5. The validation study employed elastic structural steel with the following material properties: Young's modulus E = 205.8 GPa, Poisson's ratio ν = 0.3, and yield strength σy = 313.6 MPa. Initial geometrical imperfection was incorporated following the established relationship $w0 = 0.1\beta^2 t$, where β represents the plate slenderness ratio.

Figure 4 presents the comparison between current predictions and reference results, demonstrating excellent agreement across the entire loading range. The maximum deviation in ultimate strength prediction remains below 3% for both intact and cracked configurations, validating the numerical approach's capability to capture nonlinear structural behavior accurately.

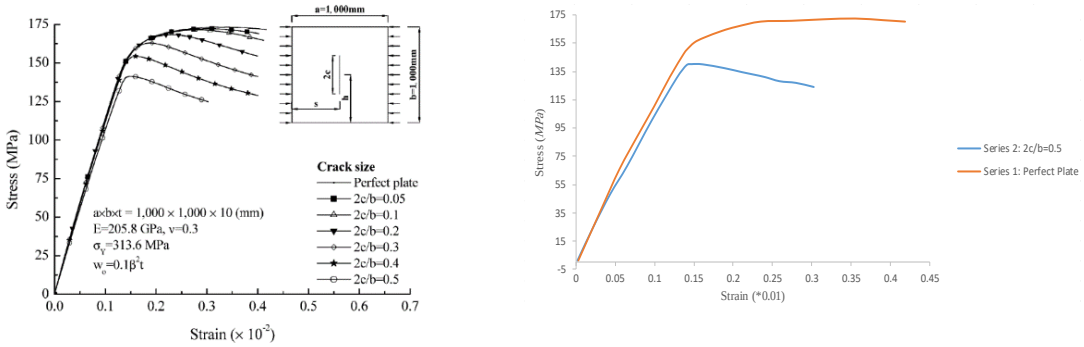

Figure 7 Comparison of predicted ultimate strength with reference FEM results [6] for intact and cracked (2c/b = 0.5) steel plates under compressive loading.

A.2 Mesh Convergence Analysis

A systematic mesh convergence study was conducted to establish optimal discretization parameters while maintaining computational efficiency. The analysis examined structural response characteristics across various mesh densities, with particular attention to stress distribution in crack-affected regions.

Figure 5 illustrates the convergence behavior of ultimate strength predictions with decreasing element size. While mesh convergence is achieved at 20 mm element size, a slightly conservative 25 mm triangular mesh was selected for the primary investigation. This choice balances numerical

accuracy with computational efficiency, ensuring reliable prediction of local stress concentrations while maintaining practical simulation times for the extensive probabilistic analysis.

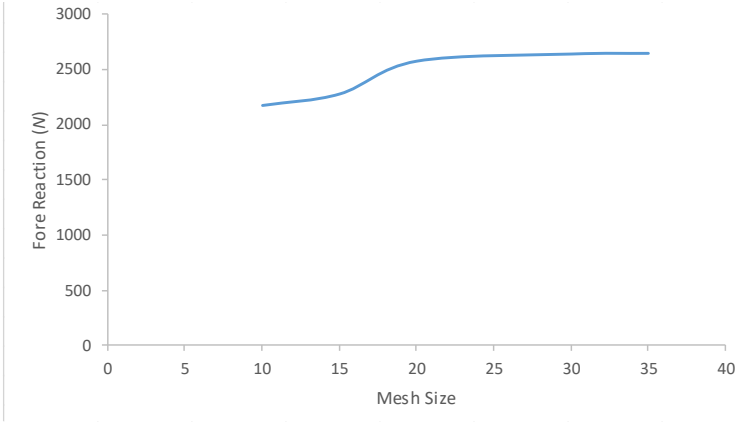

Figure 8 Mesh convergence analysis showing ultimate strength prediction versus element size, demonstrating convergence at 20 mm mesh density.

The selected mesh configuration was further validated through detailed examination of stress gradients near crack tips and comparison with analytical stress intensity predictions, confirming adequate resolution of local structural behavior.